FERRET

A FLEXIBLE NATURAL GAS MEMBRANE REFORMER FOR M-CHP APPLICATIONS

FCH JU GRANT AGREEMENT NUMBER: 621181

Start date of project: 01/04/2014 **Duration: 3 years**

WP4 – Lab-scale reformer development

D 4.4
First overall system model of novel ATR membrane reactor system

Application area: SP1-JTI-FCH.3: Stationary Power Generation & CHP
Topic: SP1-JTI-FCH.2013.3.3 Stationary Power and CHP Fuel Cell System Improvement Using Improved Balance of Plant Components/Sub-Systems and/or Advanced Control and Diagnostics Systems
Funding scheme: Collaborative Project
Call identifier: FCH-JU-2013-1

Due date of deliverable: 30-11-2015	Actual submission date: 07-12-2015	Reference period: 01-04-2014- 07-12-2015
Document classification code (*): FERRET-WP04-D44-DLR-TUE-07122015-v01.docx		Prepared by (**): TUE

Version	DATE	Changes	CHECKED	APPROVED
v0.1	07-12-2015	First Release	TUE-VS	TUE-FG

Project co-funded by the FCH JU within the Seventh Framework Programme (2007-2013)		
Dissemination Level		
PU	Public	X
PP	Restricted to other programme participants (including the Commission Services)	
RE	Restricted to a group specified by the consortium (including the Commission Services)	
CO	Confidential, only for members of the consortium (including the Commission Services)	
CON	Confidential, only for members of the Consortium	

(*) for generating such code please refer to the Quality Management Plan, also to be included in the header of the following pages

(**) indicate the acronym of the partner that prepared the document

Content

1. EXECUTIVE SUMMARY

1.1. Description of the deliverable content and purpose

The main tasks reported in this document relate to a first overall assessment of a membrane assisted fluidized bed reactor for auto-thermal reforming (MA-ATR) of natural gas and combined H_2 separation.

The energy analysis of the system is being carried out with an Aspen simulator. However, one of the outcome of this deliverable is the validation of the Aspen model with a 2 phase phenomenological model that integrates kinetics and mass transfer rates and describe the hydrodynamics of the fluidized bed membrane reactor.

The report is prepared by TUE but it is a strict collaboration between TUE and Politecnico di Milano that had a large contribution in the system evaluation.

1.2. Brief description of the state of the art and the innovation brought

First analysis of the m-CHP system with integrated fluidized bed reactors for different NG compositions.

1.3.- Deviation from objectives

N/A

1.4. If relevant: corrective actions

N/A

1.5. If relevant: Intellectual property rights

N/A

2. Introduction

In this report, a first overall assessment of a membrane assisted fluidized bed reactor for auto-thermal reforming (MA-ATR) of natural gas and combined H_2 separation is discussed. The schematic of the membrane reactor is represented in Figure 1.

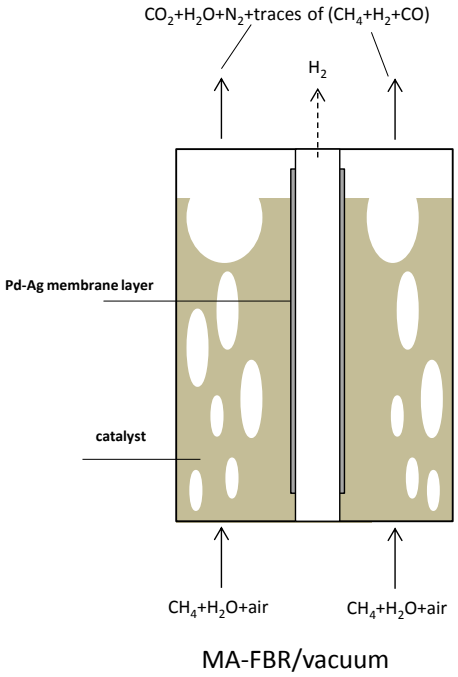

Figure 1: Membrane Assisted Fluidized Bed Reactor configuration

The MA-ATR is integrated in a stand-alone unit where pure H_2 is produced for combined heat and power generation using a PEM fuel cell. The schematic of the H_2 production process in depicted in Figure 2: natural gas from the pipeline is compressed and sent to the reactor. Air is compressed and mixed with H_2O in order to reach the required steam-to-carbon (S/C) and oxygen-to-carbon (O/C) which are calculated as follow.

$$S/C = \frac{F_{H_2O}}{\sum_{i=1}^{4} i \cdot F_{C_iH_{2i+2}}} \quad (1)$$

$$O/C = \frac{2 \cdot F_{O_2}}{\sum_{i=1}^{4} i \cdot F_{C_iH_{2i+2}}} \quad (2)$$

The air+H_2O are pre-heated up to the inlet temperature (450-550°C depending on the operating conditions of the MA-ATR) and fed to the system. In the first part of the reactor, the CH_4 reacts with O_2 and H_2O to produce some CH_4. Most of the O_2 is consumed and the some H_2 is produced due to the reforming and CH_4 partial oxidation reaction.

The H_2 permeates through the membrane at low pressure (0.3 bar) and after the first cooling it is compressed to 1 bar using a vacuum pump.

The retentate gas, which is a mixture of CO_2, H_2O and N_2 eventually with some unconverted CO, CH_4 and part of the H_2 that cannot be separated, is also used to pre-heat the air+H_2O flow rate. After cooling, it is used in a burner to complete the oxidation of the fuel species left from the MA-ATR and provide the required heat to the integrated plant.

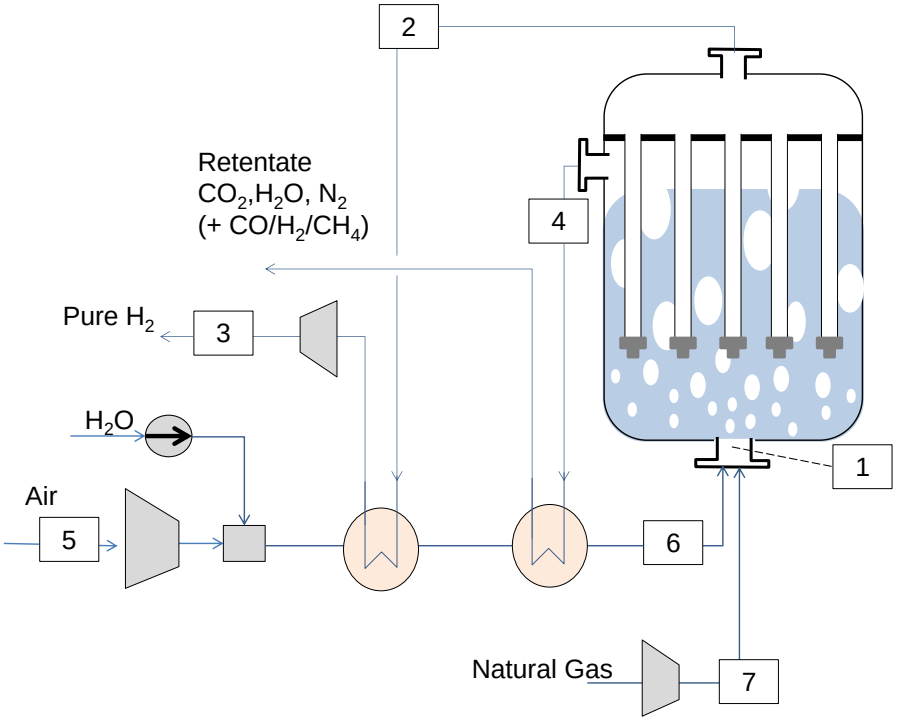

Figure 2: Process flowsheet

In this report a sensitivity analysis of the MA-ATR performance is carried out and different designs are compared. An important parameter described is Hydrogen Recovery Factor (HRF) which is defined as the ratio between permeated hydrogen and the maximum flow of hydrogen that could be produced. It is calculated as follows:

$$HRF = \frac{F_{H_2,perm}}{F_{H_2,equivalent^1}} \quad (3)$$

The main assumptions behind the analysis are summarized in the table below:

Parameter	**units**	**value**[a]
Feed & operating conditions		
Natural gas composition:		
CH_4, C_2H_6, C_3H_8, n-C_4H_{10} , i-C_4H_{10}, n-C_5H_{12}, i-C_5H_{12}, C_6H_{14}, N_2, CO_2		
81.2%,2.8%, 0.4%, 0.08%, 0.06%, 0.02%, 0.02% , 0.08%, 14.4%,0.89%		
Uniform reforming temperature	°C	600 (575-600)
Pressure reaction side	bar	8 (6-12)
Pressure permeate side	bar	0.3
S/C	-	3.0
λ_{cath} (air to cathode)	-	2
$\lambda_{ATR\text{-}MR}$ (air to ATR-MR)[b]	-	≈ 0.23

[1] $F_{H_2,equivalent^1} = \left(\sum_i^{H_nC_m} F_i \times \left(2n_i + \frac{m_i}{2}\right) + F_{CO} + F_{H_2} - 2 \times F_{O_2}\right)_{feed}$

3. Description of the models

The analysis of the system is based assuming the system under steady-state conditions and therefore any dynamic operations have been considered. The analysis is based on a pseudo-homogeneous one-dimensional model in which: i) any radial effect in the temperature profile; ii) the gas are perfectly mixed and there is any diffusion occurring from the bulk phase to the membrane surface (concentration polarization are neglected); iii) no diffusion limitations are occurring inside the catalyst.

3.1 Kinetic model

The kinetic model used for the analysis has been taken from Numaguchi and Kikuchi [1]. The reaction mechanism is based on the following three reactions:

SMR: $CH_4 + H_2O \rightleftarrows 3H_2 + CO$

MC: $CH_4 + 2O_2 \rightarrow 2H_2O + CO_2$

WGS: $CO + H_2O \rightleftarrows H_2 + CO_2$

The reaction rates R [mol $m^{-3}s^{-1}$] of the abovementioned reactions are calculated as follows (

Table 1):

Table 1: kinetic model expressions

Reaction rates expressions

$$R_{MC} = \frac{k_{a,MC}\, p_{CH4}\, p_{O2}}{\left(1 + K^{ox}_{CH4} p_{CH4} + K^{ox}_{O2} p_{O2}\right)^2} + \frac{k_{b,MC}\, p_{CH4}\, p_{O2}}{\left(1 + K^{ox}_{CH4} p_{CH4} + K^{ox}_{O2} p_{O2}\right)}$$

$$R_{SMR} = \frac{k_{SMR}\left(p_{CH4}\, p_{H2O} - p^3_{H2}\, p_{CO} / K_{eq,SMR}\right)}{p^{1.596}_{H2O}}$$

$$R_{WGS} = \frac{k_{WGS}\left(p_{CO}\, p_{H2O} - p_{H2}\, p_{CO2} / K_{eq,WGS}\right)}{p_{H2O}}$$

	Pre exponential factor	Activation energy (kJ/mol)
$k_{a,MC}\,(mol\ s^{-1} m^{-3}_{react}\ \mathrm{bar}^{-2})$	$5.51 \cdot 10^{8}$	86.0
$k_{b,MC}\,(mol\ s^{-1} m^{-3}_{react}\ \mathrm{bar}^{-2})$	$4.64 \cdot 10^{8}$	86.0
$k_{SMR}\,(mol\ s^{-1} m^{-3}_{react}\ \mathrm{bar}^{-0.404})$	$1.78 \cdot 10^{8}$	106.9
$k_{WGS}\,(mol\ s^{-1} m^{-3}_{react}\ \mathrm{bar}^{-1})$	$1.67 \cdot 10^{5}$	54.5
$K^{ox}_{CH4}\,(bar^{-1})$	$1.26 \cdot 10^{-1}$	-27.3
$K^{ox}_{O2}\,(bar^{-1})$	$7.87 \cdot 10^{-7}$	-92.8
$\ln\left(K_{eq,SMR}\right) = \frac{-20009}{T(K)} - 22.82$		
$\ln\left(K_{eq,SMR}\right) = \frac{4400}{T(K)} - 4.036$		

The expression used for hydrogen permeation is described in equation (4) where "P_{H_2}" is the pure hydrogen permeance value (mol/s.m^2.Pa^n), the term inside brackets represents the driving force for the permeation, and "n" is the exponential factor. In this work, the parameters of an asymmetric membrane, developed by Tecnalia, with a Pd layer of 4.5 μm on a ceramic support, are implemented. The

permeance is assumed equal to $P_{H_2} = 2.17 \cdot 10^{-3}\, mol/s\, m^2 Pa^{0.5}$ at 400°C with a corresponding $n = 0.5$ [2]. The initial production of hydrogen takes place in the inlet section of the reactor prior to the membranes (also referred to as pre-reforming), then in the membrane reactor section, the extraction of hydrogen through the perm-selective membrane drives the equilibrium reaction towards the products.

$$F_{H_2,perm} = \int_{A_{mem}} P_{H_2} \cdot \left({p_{H_2,ret}}^n - {p_{H_2,perm}}^n\right) dA \qquad (4)$$

The H_2 permeation has been calculated using the Sievert's law the membrane permeability has been calculated according to experimental data.

The H_2 flux (ϕ''_{H2}) through the membrane is calculated as:

$$\phi''_{H2}(mol\, m^{-2} s^{-1}) = \frac{P_m}{t}\left(p^{0.5}_{H2,ret} - p^{0.5}_{H2,perm}\right)$$

3.2 Hydrodynamics and mass transfer model

The membrane assisted fluidized bed model merged the concept of reaction kinetics with bed hydrodynamics and gas separation. A one dimensional two-phase fluidization model is considered for the simulation of fluidized bed membrane reactor. This model has been developed in the past years and used for different process involving H_2/O_2 membrane reactors [3,4]. There are two phase considered in the reactor i.e. bubble and emulsion phase. The schematic of the reactor is a combination of different continuous stirred tank reactors (CSTRs) each section consists of further sub CSTRs. The bubble phase is simulated as a pseudo-PFR and therefore the number of CSTR is increased as shown in Figure 3. The H_2 permeates through the membrane from both the emulsion and the bubble phase, which however are working with a different gas composition due to the mass transfer of the system. For the MA-ATR, the energy balance is accounted only for the overall system and it is not implemented in the model. For this reason, the analysis is carried out at iso-thermal conditions and the correct temperature of the system is assessed from an external calculation after knowing the hydrogen the final gas composition at the retentate and at the permeate sides and considered the amount of H_2 that has been separated.

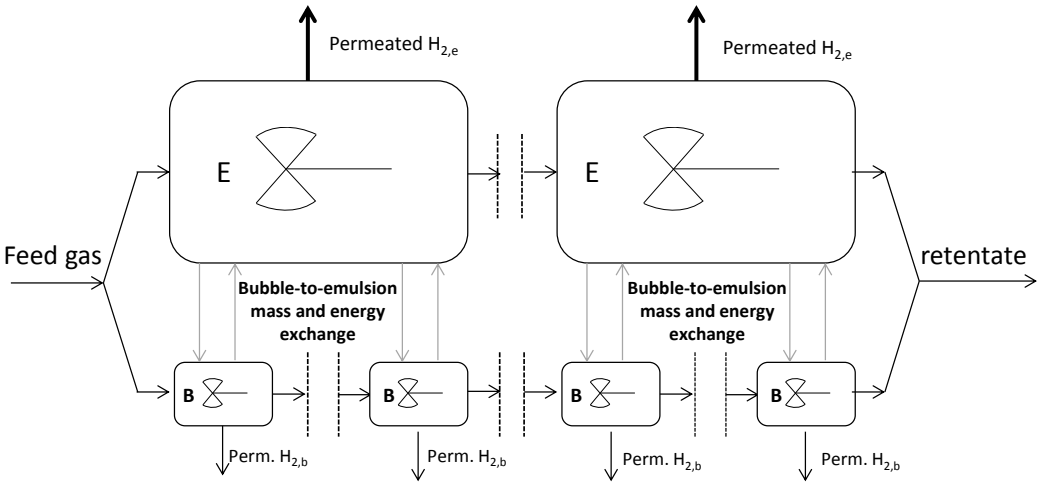

Figure 3: Schematic of the MA-FBR model

Moreover, the model also assumes that the gas passing through the emulsion phase is at minimum fluidization velocity and is properly mixed in each section while the remaining gas flows as bubbles. The gas permeated from both bubble and emulsion phase through membrane is distributed on the basis of local bubble fractions. Meanwhile, the gas separated from emulsion phase is immediately compensated through bubble phase (to keep the emulsion phase at minimum fluidization). The gas compensated

through bubbles phase is depends on the value of bed voidage (bed expansion). The bed voidage (ε) represents the division of membrane area between bubble and emulsion phase. The bubbles are free of catalyst, both the reactions i.e. SMR and WGS are happening in the emulsion phase. A constant temperature is considered across the reactor bed with no heat loses to the surroundings. The correlations and equations used in the modelling are shown in
Table 2.

Table 2: Hydrodynamic parameters used in the modelling

Parameters	Equation	Ref.
Archimedes number	$Ar = {d_p}^3 \rho_g(\rho_p - \rho_g)g/{\mu_g}^2$	[5]
Minimum fluidization velocity	$u_{mf} = (\mu_g/d_p\rho_g)\left(\sqrt{(27.2)^2 + 0.0408Ar} - 27.2\right)$	[6]
Bed voidage at minimum fluidization velocity	$\varepsilon_{mf} = 0.586Ar^{-0.029}\left(\frac{\rho_g}{\rho_p}\right)^{0.021}$	[6]
Velocity of rise of swarm of bubbles	$u_b = u_o - u_{mf} + u_{br}$	[5]
Rising velocity of single bubble	$u_{br} = 0.711(g d_{b,avg})^{1/2}$	[5]
Emulsion velocity	$u_e = \frac{u_o - \delta u_b}{1 - \delta}$	[5]
Average bubble diameter	$d_{b,avg} = d_{b,max} - (d_{b,max} - d_{bo})\exp\left(-\frac{0.3H}{D_T}\right)$	[7]
Initial bubble diameter	$d_{bo} = 0.376(u_o - u_{mf})^2$	[4]
Bubble phase fraction	$\delta_{bn} = \frac{{u_b}^s}{u_b}$	[4]
Emulsion phase fraction	$\delta_{en} = 1 - \delta_{bn}$	[4]
Maximum superficial bubble gas velocity	${u^s}_{b,max} = u_o - u_{mf}$	[4]
Initial superficial bubble gas velocity	${u^s}_{b,o} = u_{br,o}\delta_{bo}$ where $\delta_{bo} = (1 - H_{mf}/H_f)$	[4]
Height of bed at minimum fluidization velocity	$H_{mf} = H_s\frac{1 - \varepsilon_s}{1 - \varepsilon_{mf}}$	[7]
Height of bed expansion	$H_f = H_{mf}\frac{C_1}{C_1 - C_2}$ where, $C_1 = 1 - \frac{u_{b,o}}{u_{b,avg}}exp\left(-\frac{0.275}{D_T}\right)$ $C_2 = \frac{{u_b}^s}{u_{b,avg}}\left[1 - exp\left(-\frac{0.275}{D_T}\right)\right]$	[4]
Average bubble rise velocity	$u_{b,avg} = u_o - u_{mf} + 0.711(g d_{b,avg})^{1/2}$	[4]
Gas exchange coefficient	$K_{bc} = 4.5\left(\frac{u_{mf}}{d_p}\right) + 5.85\left(\frac{{D_g}^{1/2}g^{1/4}}{{d_b}^{5/4}}\right)$ $K_{ce} = 6.77\left(\frac{D_g\varepsilon_{mf}u_b}{{d_b}^3}\right)^{1/2}$ $\frac{1}{K_{be}} = \frac{1}{K_{bc}} + \frac{1}{K_{ce}}$	[4]

4. Results

The analysis has been carried out keeping the reactor inlet flow constant and varying respectively u/u_{mf} and the free space reactor diameter D_t.

A first comparison has been made at ideal conditions with reactions at equilibrium conversion and absence of mass transfer limitations. In these conditions, as expected, the two models give identical performances in terms of H_2 extraction and NG conversion where the choice of different u/u_{mf}, D_t do not affect the results.

The following simulations have been performed introducing first the kinetic rate limitations (KL), then the emulsion-to-bubble mass transfer limitations (MTL) and finally coupling these two effects (KL+MTL). The reactor design implemented in the 1D two-phase model consider the presence of 12 membranes with an outer diameter of 0.1 m and a length of about 0.38 m. Membranes are arranged in order to keep a distance of 0.025 m each other, i.e. Figure 4.

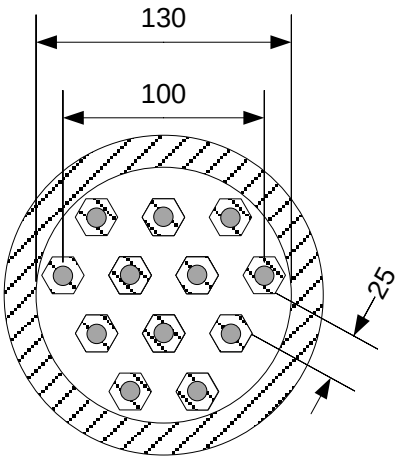

Figure 4: Example of membrane reactor cross-section

Figure 5 points out that the kinetic rate limitations do not have a big impact on the reactor performances since the oxidation and reforming reactions are however faster in comparison to species mass transfer limitation.

Results of the phenomenological model show an H_2 permeation flow of 3.1 Nm^3/h at u/u_{mf} 2.5 that corresponds to the 86% of the amount obtained with the quasi-lumped model. The maximum H_2 extraction value cannot be taken into account because the inlet feed velocity is not high enough to sustain the fluidization regime along the entire membrane reactor. The gap between the two models (14%) can be reduced up to 8% increasing to 2 times the original membrane area (CH_4 conversion reach 94.5%), or up to 6% increasing to 5 times the membrane area (CH_4 conversion at 95%).

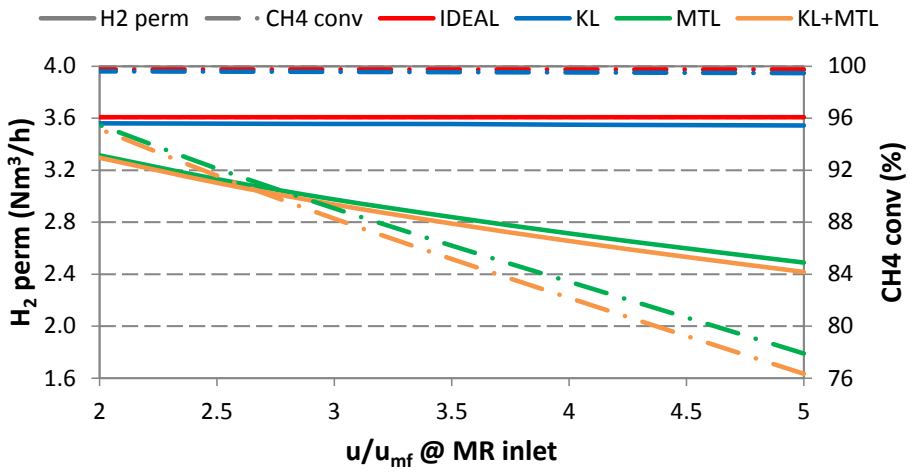

Figure 5: MR Model comparison for the worst case: H_2 permeation and CH_4 conversion from ideal to kinetic and mass transfer limitations conditions.

Regarding the bubble break-up case, setting the limit to the growing of the bubble size in the maximum bubble diameter relation [5] is reasonable if the reactor contains internals (membranes). In this work the limit is set as the maximum distance between membranes (0.025 m) as described in the following equation:

$$d_{b,max} = min\left(0.025\,, 0.65\frac{\pi}{4}D_t^2(u_0 - u_{mf})\right) \quad (5)$$

Moreover, Figure 6 shows a comparison of the reactant composition along the membrane reactor founded by the two models where the 1D model works at u/u_{mf} equal to 3 under the bubble break-up assumption. The solid lines are representative for the quasi-lumped model while the dotted lines are related to the phenomenological model results.

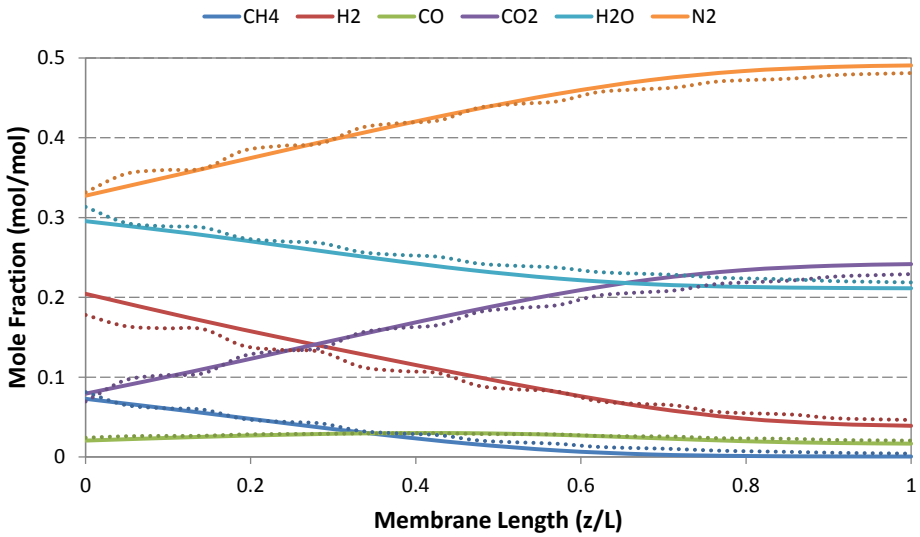

Figure 6: Example of reactant composition along the membrane reactor: solid line is the quasi-lumped model and the dotted line is the 1D two-phase model (u/u_{mf} = 3; break-up bubble case).

For this case the mass and the energy balances of the simplified system is reported in Table 3 and table Table 4.

Table 3: Energy Balance of the MA-ATR

	units	
S/C[2]	-	3
Temperature reactor	°C	600
Pressure reaction side	bar	8
S/C ratio at inlet of ATR-MR	-	1.80
O/C ratio at inlet of ATR-MR	-	0.93
NG feed	Nm^3/h	1.44
NG power input [LHV base]	kW	12.68
NG power input [HHV base]	kW	14.05
NG compressor	kW	0.17
Air compressor	kW	0.36

[2] S/C takes into account also the amount of H_2O produced during the combustion with O_2.

Vacuum pump	kW	0.26
Total membrane area	m^2	0.141
Hydrogen permeation	Nm^3/h	3.61
Hydrogen Recovery Factor	%	93

Table 4: Main Thermodynamic points of the streams selected in Figure 2

	F	m	T	p	composition (% vol.)													
	mol/s	kg/s	°C	mbar	CH4	C2H6	C3H8	C4H10-01	C4H10-02	C5H12-01	C5H12-02	C6H14	H2	CO	CO2	H2O	O2	N2
1	0.08251	1.88E-03	432.9	8000	0.17626	0.00618	0.0008	0.000174	0.00013	4.34E-05	4.34E-05	0.00017	0.000	0.000	0.002	0.354	0.090	0.371
2	0.04471	9.01E-05	600.4	300	0.000	0.000	0.000	0.000	0.000	0.000	0.000	0.000	1.000	0.000	0.000	0.000	0.000	0.000
3	0.04471	9.01E-05	70.0	1200	0.000	0.000	0.000	0.000	0.000	0.000	0.000	0.000	1.000	0.000	0.000	0.000	0.000	0.000
4	0.06226	1.79E-03	600.0	8000	5.80E-04	0.000	0.000	0.000	0.000	0.000	0.000	0.000	0.038	0.017	0.242	0.212	0.000	0.491
5	0.0359	1.03E-03	15.0	1013	0.000	0.000	0.000	0.000	0.000	0.000	0.000	0.000	0.000	0.000	0.000	0.013	0.207	0.780
6	0.0646	1.55E-03	557.2	8000	0.000	0.000	0.000	0.000	0.000	0.000	0.000	0.000	0.000	0.000	0.000	0.451	0.115	0.433
7	0.0179	3.34E-04	107.8	8000	0.812	0.029	0.004	0.001	0.001	0.000	0.000	0.001	0.000	0.000	0.009	0.000	0.000	0.144

5. References

[1] T. Numaguchi, K. Kikuchi, Intrinsic kinetics and design simulation in a complex reaction network; steam-methane reforming, Chem. Eng. Sci. 43 (1988) 2295–2301.

[2] E. Fernandez, A. Helmi, K. Coenen, J. Melendez, J.L. Viviente, D.A. Pacheco Tanaka, et al., Development of thin Pd–Ag supported membranes for fluidized bed membrane reactors including WGS related gases, Int. J. Hydrogen Energy. 40 (2015) 3506–3519.

[3] F. Gallucci, M. Annaland, J. Kuipers, Autothermal reforming of methane with integrated CO2 capture in a novel fluidized bed membrane reactor. Part 1: experimental demonstration, Top. Catal. 51 (2008) 133–145.

[4] F. Gallucci, M. van Sint Annaland, J. Kuipers, Autothermal reforming of methane with integrated CO2 capture in a novel fluidized bed membrane reactor. Part 2 comparison of reactor configurations, Top. Catal. 51 (2008) 146–157.

[5] D. Kunii, O. Levenspiel, Fluidization Engineering, Elsevier, 1991.

[6] C.-Y. Shiau, C.-J. Lin, Equation for the superficial bubble-phase gas velocity in fluidized beds, AIChE J. 37 (1991) 953–954.

[7] S. Mori, C.Y. Wen, Estimation of bubble diameter in gaseous fluidized beds, AIChE J. 21 (1975) 109–115.